Competitive Adsorption from Mixed Hen Egg-White Lysozyme/Surfactant Solutions at the Air−Water Interface Studied by Tensiometry, Ellipsometry, and Surface Dilational Rheology

V. S. Alahverdjieva,*,† D. O. Grigoriev,† V. B. Fainerman,‡ E. V. Aksenenko,§ R. Miller,† and H. Möhwald†

Max-Planck-Institut für Kolloid- und Grenzflächenforschung, Am Mühlenberg 1, 14424 Potsdam, Germany, Medical Physicochemical Centre, Donetsk Medical University, 16 Ilych Avenue, 83003 Donetsk, Ukraine, and Institute of Colloid Chemistry and Chemistry of Water, 42 Vernadsky Avenue, 03680 Kyiv (Kiev), Ukraine

Received: June 19, 2007; In Final Form: November 13, 2007

The competitive adsorption at the air−water interface from mixed adsorption layers of hen egg-white lysozyme with a non-ionic surfactant (C_{10}DMPO) was studied and compared to the mixture with an ionic surfactant (SDS) using bubble and drop shape analysis tensiometry, ellipsometry, and surface dilational rheology. The set of equilibrium and kinetic data of the mixed solutions is described by a thermodynamic model developed recently. The theoretical description of the mixed system is based on the model parameters for the individual components.

Introduction

The adsorption from mixed protein/surfactant solutions at the air−water interface has many important technological applications, for example, for stabilization of emulsions and foams in the food industry, cosmetics, coating processes, oil recovery, and so forth.[1−5] In many foamed or emulsified foodstuffs, proteins as well as low-molecular-weight surfactants are present. Both types of molecules are surface-active but with different roles for the stabilization of foams and emulsions. Low-molecular-weight surfactants stabilize dispersed systems via the Marangoni mechanism, and, namely, they tend to move away from a region of the surface layer, where the surface tension is locally lowered in order to annihilate the surface-tension gradient. On the contrary, polymers, including proteins, are most effective for stabilizing dispersed systems due to steric effects and the formation of strong viscoelastic adsorbed layers.

The adsorption kinetics from mixed protein/surfactant solutions can be studied via two different experimental approaches—sequential adsorption and simultaneous adsorption. In the former case, one lets the protein first adsorb at the interface, for example, in a drop experiment, or spreads it at the surface of a Langmuir trough[6−8] and then injects the surfactant either by means of a double capillary in single-drop experiments[9] or by a syringe into the bulk phase in a trough experiment. This way of performing the experiment guarantees an already formed protein layer, the stability of which depends on several factors, like the time required to reach the equilibrium and the initial bulk concentration of the protein. It should be noted that a subsequent penetration of surfactant into the pre-adsorbed protein layer does not lead to an equilibrium state of the mixed adsorption layer within a realistic time scale due to high activation energy of the required protein desorption process.[10]

The second approach is more "realistic", since many biological and technological systems already contain mixtures of protein and surfactant. For example, blood serum is a mixture of human serum albumin with a number of compounds, among which are low-molecular-weight surfactants; human saliva contains a mixture of several enzymes, α-amylase, lysozyme with electrolytes, and glycoproteins; and human digestive fluids contain a mixture of enzymes and hydrochloric acid.[11]

In the case of protein/non-ionic surfactant mixtures, there is a competitive adsorption.[6−8,12−14] During the initial stage of the adsorption process, the rate of adsorption of surface-active constituents is proportional to their concentration in the solution.[1] Therefore, if the surfactant concentration is essentially higher than the protein concentration, the surfactant is first adsorbed, and then it can be displaced by the more surface-active substance, the protein. This process can attain equilibrium due to the low activation energy of surfactant desorption.[10] After a certain concentration of surfactant, the two $\gamma-c$ isotherms of the mixture and of the pure surfactant overlap, indicating a surface layer covered by free surfactant molecules.

In the case of protein/ionic surfactant mixtures, the interaction mechanism is different.[15,16] With increasing surfactant concentrations, electrostatic interactions dominate until the available charges in the protein molecule are compensated by the surfactant ions, thus forming electroneutral complexes of higher surface activity as compared with the native protein.[16] Upon further increase in surfactant concentration, hydrophobic interactions become more important, making the complex step by step more hydrophilic and less surface-active, as explained below. Due to competition in the adsorption layer, the protein/surfactant complexes which are less surface-active, become incapable of displacing the free surfactant molecules adsorbed earlier (because their concentration in the solution is high) so that finally, usually at the cmc of the surfactant, the adsorption layer is formed mainly by surfactant molecules.

In this study the second approach is presented using three essentially different experimental methods—tensiometry, ellipsometry, and surface dilational rheology—to characterize the differences in competitive adsorption from mixed protein/surfactant solutions depending on the nature of the surfactant.

* Corresponding author. E-mail: Veneta.Alahverdjieva@mpikg.mpg.de.
† Max-Planck-Institut für Kolloid- und Grenzflächenforschung.
‡ Donetsk Medical University.
§ Institute of Colloid Chemistry and Chemistry of Water.

10.1021/jp074753k CCC: $40.75
Published on Web 01/29/2008

The competitive adsorption depends not only on the nature of the low-molecular-weight surfactant—non-ionic or ionic—but also on its bulk concentration.

Materials and Methods

Materials. *Proteins*. The protein used in this study is hen egg-white lysozyme, L-6876, MW ~ 14300 g/mol (obtained from Sigma and used without further purification, stored at −20 °C). Lysozyme has an isoelectric point around 11, thus at pH 7, the pH at which the study was made, it is positively charged. Lysozyme is a rigid globular protein with dimensions of approximately 3 nm × 3 nm × 4.5 nm.

Surfactants. The surfactants used are the non-ionic C_{10}DMPO (decyl dimethyl phosphine oxide, MW = 218 g/mol, cmc = 4×10^{-3} mol/L in buffer) and the ionic SDS (sodium dodecyl sulfate, MW = 288 g/mol, cmc = 5×10^{-3} mol/L in buffer).

Solution Preparation. All the solutions for the pure components and for the mixed protein/surfactant solutions are prepared in phosphate buffer (NaH_2PO_4/Na_2HPO_4, Fluka) with pH 7 and ionic strength 10 mM using Millipore water. The surface tension of the buffer solution at 21 °C was 72.7 mN/m. The mixed protein/surfactant solutions were prepared at constant protein concentration of 7×10^{-7} mol/L and varying the surfactant concentration (for C_{10}DMPO from 10^{-5} to 9×10^{-3} mol/L, above the cmc, and in a broader concentration range for SDS from 10^{-} to 10^{-2} mol/L, again above the cmc). For the mixture of lysozyme with C_{10}DMPO, 0.5 g/L NaN_3 was added to the buffered solution in order to prevent bacterial degradation processes; for the mixture of lysozyme with SDS, sodium azide was not added, as it is known that SDS itself prevents bacterial contamination. All solutions were freshly prepared before each experiment.

Methods. *Tensiometry—Profile Analysis Tensiometry*. The dynamic surface tension at long adsorption times (from seconds to hours) was measured using the Profile Analysis Tensiometer, PAT 1 (SINTERFACE Technologies, Germany).[17] The principle of this method is to determine the surface tension of the studied solution from the shape of a pendant drop or buoyant bubble according to the Gauss-Laplace equation. Due to the active control loop, the instrument allows long-time experiments with a constant drop volume (area).[17]

In this study. the dynamic surface tension of all the solutions was monitored for 20 h at a constant area of the pendant drop. After this period, quasi-equilibrium conditions were established and the dilational rheology experiments were performed (see below).

Dilational Rheology. The experiment on the pendant drop was also used to measure the dilational viscoelasticity of the system. In this kind of experiment the area of the drop is varied in periodic harmonic oscillations with a defined input frequency and the corresponding response of the interfacial tension is measured. The oscillation of a drop or bubble leads to dilation and compression of the interface. The surface dilational modulus ϵ in compression and expansion is defined by

$$\epsilon \equiv \frac{d\gamma}{d \ln A} \tag{1}$$

where γ is the surface tension, and A is the surface area under deformation. In the simplest case, when exchange of surfactant with the adjacent bulk solution can be neglected (i.e., $\Gamma \times A$ is constant) the modulus is purely elastic, with a limiting value ϵ_0, which can be determined from the surface equation of state, that is, from the equilibrium relationship between surface tension and surfactant adsorption, Γ: [18−20]

$$\epsilon_0 = -\left(\frac{d\gamma}{d \ln \Gamma}\right)_{eq} \tag{2}$$

Deviations from this simple limit occur when relaxation processes in or near the surface affect γ and Γ.[21] In such cases, ϵ is the complex viscoelastic modulus, with a real part ϵ' (the storage modulus) and the imaginary part ϵ'' (the loss modulus). Elastic and viscous contributions can be measured separately by subjecting the surface to small periodic compressions and expansions at a given frequency. The real part, ϵ', of the complex modulus is equal to the elasticity, ϵ_d, and the imaginary part, ϵ'', is related to the viscosity, η_d, and the imposed angular frequency, ω, of the area variations:[18−21]

$$\epsilon = \epsilon' + i\epsilon'' = \epsilon_d + i\omega\eta_d \tag{3}$$

After equilibrium of the dynamic surface tension has been established, harmonic surface area perturbations are imposed. The frequencies chosen are the following: 0.01, 0.02, 0.04, 0.08, 0.16, 0.2, 0.28, and 0.4 Hz. These low frequencies guarantee slow area perturbations, so that the drop maintains its Laplacian shape, as demonstrated in ref 35. Also, the surface area change is below 10% in order to follow linear hydrodynamic behavior. In the end, Fourier analysis is performed, and as an output one obtains the dilational elasticity and dilational viscosity.

Ellipsometry. In order to measure the adsorption layer thickness and the adsorbed amount, ellipsometry measurements are performed with an instrument from Optrel, Germany. The scheme of this apparatus and the procedure to calculate layer thickness and adsorbed amount are described in detail elsewhere.[22,23] Briefly, a conventional PCSA (polarizer−compensator−sample−analyzer) null-ellipsometer setup is used. A low-capacity laser with $\lambda = 532$ nm serves as a light source (beam diameter about 0.5−1 mm). The light beam passes through a first quarter-wave plate to produce a circularly polarized light. Then the light is linearly polarized by the polarizer (a Glan-Thompson prism) mounted in a rotatable divided circle, which can be read with very high precision. A second quarter-wave plate (the compensator) and the analyzer (a second Glan-Thompson prism) are mounted in a similar manner. The angle of incidence of the light is 50°. As a detector, a photodiode is used. Both incidence and reflection arms are motorized and computer-controlled. The highly precise motors of the polarizer and the analyzer, also computer-controlled, allow the exact determination of the null positions (positions at which a minimal intensity of transmitted light is registered) of both optical elements. From the nulls of the polarizer and the analyzer, two ellipsometric angles, Δ and Ψ, can be obtained. These angles characterize the polarization state of reflected light, which can be attributed to the properties of the reflecting surface.[23] In the case when the adsorbed layer is relatively thick and not homogeneous in the bulk (substrate) normal to the interface, the refractive index n_1 and thickness d_1 of the film as calculated from the experimental values of $\delta\Psi$ and $\delta\Delta$ represent optical averages (denoted by $\bar{n}_1$ and $\bar{d}_1$). The refractive index in the adsorbed layer n_1 depends linearly on the solute concentration $n_1 = n_2 + (dn/dc)(c(z) - c(\infty))$, where n_2 is the refractive index in the substrate and $c(z)$ is the solute concentration in the layer as a function of the distance from the interface ($z = 0$) to the bulk and c (∞) is the solute concentration in the bulk solution. Under these assumptions, the adsorption Γ can be calculated from the mean layer thickness $\bar{d}_1$ and the average refractive index $\bar{n}_1$:

$$\Gamma = \frac{\bar{d}_1(\bar{n}_1 - n_2)}{\mathrm{d}n/\mathrm{d}c} \quad (4)$$

where dn/dc is the refractive index increment, which for lysozyme is 0.186.[36]

Results and Discussions

The results of theoretical and experimental studies of dynamic and equilibrium surface tension and adsorption (ellipsometry method) of individual lysozyme solutions were discussed recently in ref 24 using a theoretical model for the adsorption of proteins in multiple states, derived by Fainerman et al.[25,26] This model was generalized to describe also multilayer adsorption.[38] For the sake of clarity, a brief description of the model will be given here. Within the framework of a nonideal two-dimensional solution model, equations are derived for the state of the surface layer, adsorption isotherms, and the distribution function of adsorbed protein molecules with respect to their surface states characterized by different molar surface areas. According to this thermodynamic adsorption model, the protein molecule can exist in the surface layer in various states with different molar surface areas varying from a maximal value, ω_{max} (at very low surface coverage, low surface pressure) to a minimal value, ω_{min} (at very high surface coverage, high surface pressure); the molar surface area of the solvent ω_0 is assumed to be much smaller than ω_{min}. The protein molecules having different states coexist at the surface and are at equilibrium with each other. This model takes into consideration also the mutual interactions between the adsorbed species, characterized by the constant a. The surface activity of the adsorbing protein molecules in a certain j^{th} state is expressed by the adsorption equilibrium constant b_j. The model further assumes that for all j-states b_j are equal to each other; therefore the adsorption equilibrium constant for a protein molecule as a whole is equal to $b = \sum b_j = nb_j$. Taking into account that b_j = constant, the distribution function of the adsorption values of protein in different states can be derived.[25,26] At very high protein concentrations (above a critical concentration c^*), the surface tension of the solution is almost constant; however the adsorption still increases. After a certain critical surface pressure π^* or critical adsorption Γ^*, the approximately constant value of π may be explained by the changes in surface layer, for example, two-dimensional condensation or compression of molecules and by the formation of a second adsorption layer. All this leads to a change in the average molar surface area of the protein, and an additional parameter ϵ is introduced to account for the relative compressibility of the protein molecule above a critical concentration.

The expressions for the protein/surfactant layers are derived in a similar manner.[16,45]

The studies of the dynamic and equilibrium surface tension of mixed solutions of lysozyme (7×10^{-7} mol/L) with SDS are discussed in ref 27 on the basis of a model which assumes the formation of complexes between ionized protein molecules and ionic surfactants.[16] In the present discussion, we make use of the results reported in refs 24 and 27. A summary of the relevant adsorption parameters used is given in Table 1.

The data given below will be discussed on the basis of theoretical models developed recently for mixtures of proteins and non-ionic[14] and ionic surfactants[16] in analogy with the thermodynamic model for pure proteins derived in refs 25 and 26. Due to the rather large complexity of the respective sets of equations, we will not repeat them here. The dynamics of adsorption, measured here in terms of dynamic surface tensions, has been interpreted using a diffusion-controlled adsorption mechanism, assuming that the process of adsorption from the subsurface is fast compared to the diffusion from the bulk. The theoretical model comprises two equations of the Ward and Tordai type, one for each compound, interrelated via the respective mixed adsorption isotherm.[39]

TABLE 1: Adsorption Parameters of Lysozyme, Lysozyme/C_{10}DMPO, and Lysozyme/SDS Used in the Model Calculations[a]

adsorption parameters	
Protein-Specific Parameters	
a	0.69
ω_0, m^2/mol ($\times 10^5$)	4.95
ω_1, m^2/mol ($\times 10^6$)	7.72
ω_{max}, m^2/mol ($\times 10^7$)	2.54
ϵ	0.25
π^*, mN/m	14.5
b_1, m^3/mol	1×10^4
b_2, m^3/mol	30
C_{10}DMPO-Specific Parameters	
ω_S, m^2/mol ($\times 10^5$)	3
b_S, m^3/mol	7.23×10^1
SDS-Specific Parameters	
ω_S, m^2/mol ($\times 10^5$)	2.85
b_S, m^3/mol	1.9×10^1
m	8

[a] ω_0 = molar area of the solvent; ω_1 = minimal molar area; ω_{max} = maximal molar area; a = intermolecular interaction parameter; b = adsorption equilibrium constant; e = parameter accounting for the internal compressibility; π^* = critical surface pressure; m = parameter accounting for the number of charges in the protein molecule available for electrostatic interactions with oppositely charged surfactant; the subscript "S" refers to the surfactant.[25,26]

The quantitative analysis of data from dilational rheology experiments (oscillating drop studies) requires also a respective theoretical model. This model represents a generalization of the theory proposed first by Lucassen and van den Tempel[18,19] to mixed solutions as discussed in detail recently elsewhere.[28]

The dynamic surface tension for 7×10^{-7} mol/L lysozyme/C_{10}DMPO and 7×10^{-7} mol/L lysozyme/SDS is measured using the Profile Analysis Tensiometer on the surface of a pendant drop for 20 h in water-saturated atmosphere to prevent possible evaporation. The results are shown in Figures1 and 2, respectively. A red solid line shows the dynamic surface tension for pure 7×10^{-7} mol/L lysozyme. The time axis is presented on a logarithmic scale in order to draw the attention to a kinetic feature, characteristic for many different proteins, the so-called induction period. This term describes the beginning of the pronounced decrease of the surface tension. The general physical picture of the induction period is that there is a minimum adsorption of the protein necessary until the surface tension starts decreasing,[24,37] or in other words, until a measurable two-dimensional surface pressure occurs. This induction period is observable as a break in the slope of the surface tension versus time for concentrations below 5×10^{-5} mol/L. For lysozyme, which is a robust globular protein, this induction period is even longer as compared to other proteins, for example, the flexible β-casein, which implies that the protein not only has to adsorb, but also subsequently must unfold partially at the interface in order to produce a measurable surface pressure. Apparently, the lower is the bulk concentration the poorer is the flexibility of the protein, and hence with lower ability to unfold the longer is the induction period.

The dynamic surface tension curves in Figure 1 show that a significant change in surface tension induced by the addition of surfactant is observed when the surfactant concentration is

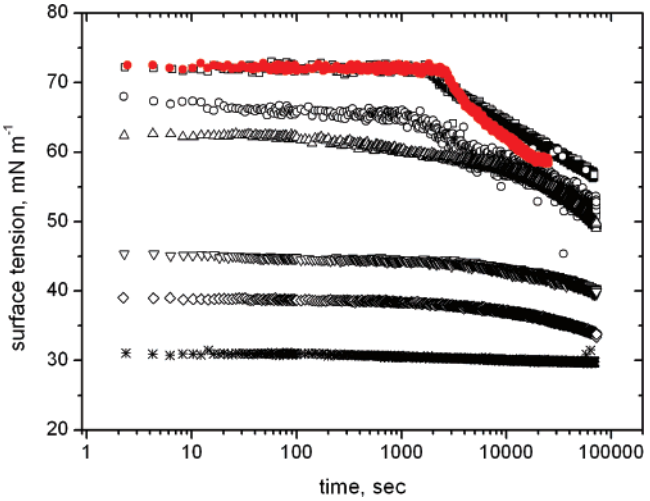

Figure 1. Figure 1. Dynamic surface tension of 7×10^{-7} mol/L lysozyme−C_{10}DMPO solution at the air−water interface measured with the pendant drop method for different C_{10}DMPO concentrations: □, 10^{-9} mol/L; ○, 5×10^{-5} mol/L; △, 10^{-4} mol/L; ▽, 10^{-3} mol/L; ◇, 2×10^{-3} mol/L; and ∗, 9×10^{-3} mol/L.

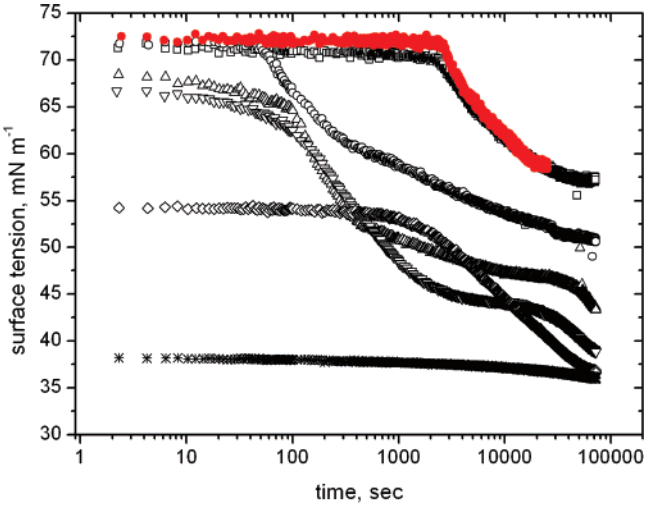

Figure 2. Dynamic surface tension of 7×10^{-7} mol L^{-1} lysozyme−SDS at the air−water interface measured with the pendant drop method for different SDS concentrations: □, 10^{-9} mol/L; ○, 10^{-6} mol/L; △, 5×10^{-5} mol/L; ▽, 10^{-4} mol/L; ◇, 10^{-3} mol/L; and ∗, 10^{-2} mol/L.

above 10^{-5} mol/L. The equilibrium surface tension, reached at the highest studied surfactant concentration (9×10^{-3} mol/L) is about 29 mN/m which corresponds to the equilibrium surface tension of the critical micelle concentration of pure C_{10}DMPO.

When SDS is added to a 7×10^{-7} mol/L lysozyme solution, Figure 2, the picture is quite different. A significant change in the surface tension behavior as compared to the pure lysozyme is observed at much lower concentrations in comparison to C_{10}-DMPO. At SDS concentrations higher than 10^{-6} mol/L, the shape of the dynamic surface tension curves in Figure 2 becomes essentially more complicated. An additional significant surface tension decrease at longer times indicates that the adsorption of lysozyme/SDS complexes takes place, as these complexes are much more surface-active than the native lysozyme molecules. Further increase of SDS concentration does not lead to any appreciable additional decrease of the surface tension in the long time range, because here the lysozyme adsorption is low. The highest concentration, 1×10^{-2} mol/L, which is just above the critical micelle concentration of SDS, yields dynamic surface tensions completely controlled by the surfactant. From Figures 1 and 2, it becomes evident that one has to measure over very long times to arrive at equilibrium values.

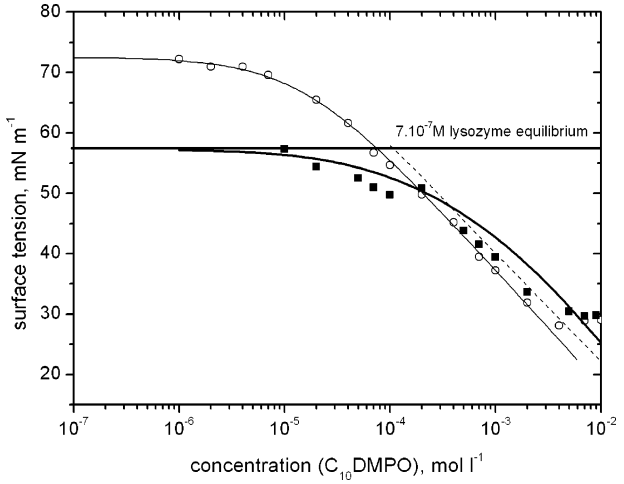

Figure 3. Equilibrium surface tension isotherm for C_{10}DMPO (○) and 7×10^{-7} mol/L lysozyme/C_{10}DMPO (■) at the air−water interface; lines are theoretical curves. Thin solid line: Langmuir model with $\omega_S = 2.94 \times 10^5$ m²/mol, $b_S = 68$ m³/mol and internal compressibility $\epsilon_S = 0.012$ m/mN; thick solid line: theoretical fit of the mixture using the model[25,26] and model parameters in ref 24; dashed line: theoretical fit of the mixture[24−26] with $b_P = 10^4$ m³/mol.

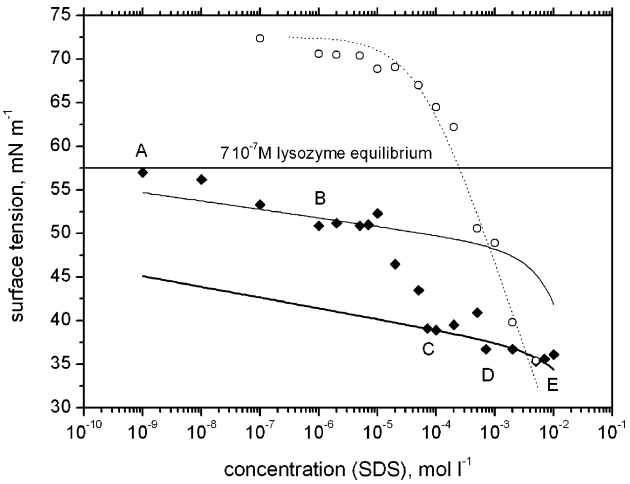

Figure 4. Equilibrium surface tension isotherm for SDS (○) and 7×10^{-7} mol/L lysozyme−SDS (◆) at the air−water interface, lines represent the theoretical curves. Dotted line: Langmuir model with $\omega_S = 2.85 \times 10^5$ m²/mol, $b_S = 19$ m³/mol, and internal compressibility $\epsilon_S = 0.012$ m/mN; thin solid line: theoretical fit of the mixture using the model[25,26] and model parameters corresponding to set 2 of ref 27; bold solid line: theoretical fit of the mixture using the model[25,26] and model parameters corresponding to set 5 of ref 27.

The surface tension isotherm for lysozyme/C_{10}DMPO is presented in Figure 3, and the one for lysozyme/SDS is presented in Figure 4. The equilibrium surface tensions are estimated from the extrapolation of the dynamic data for $t \rightarrow \infty$ using the plot $\gamma = \gamma(t^{-1/2})$. This extrapolation corresponds to the consideration of a diffusion-controlled adsorption mechanism. To be able to make a comparison with the pure surfactants, the concentrations of which are varied in the mixed solution, their isotherms are also shown. As the concentration of the protein in the mixtures does not change (it is kept constant), it is presented as a straight solid line in both figures. The two isotherms for the mixed protein/surfactant solutions look distinctively different, making it evident that the competitive

adsorption depends strongly on the nature of the surfactant. Let us consider first the competitive adsorption when a non-ionic surfactant is added to the protein solution, Figure 3. From the surface tension isotherm, one can see that the adsorption layer is dominated by both the protein and the surfactant up to concentrations around 2×10^{-4} mol/L. At higher concentrations of C_{10}DMPO, the two surface tension isotherms practically overlap, which indicates that the adsorption layer is covered mainly by free surfactant molecules. This fact could possibly be attributed not only to the essential increase of the surfactant concentration but also (at least partially) to the protein hydrophilization due to the hydrophobic binding of C_{10}DMPO molecules.

Figure 3 also presents the theoretical dependencies of the surface tension for lysozyme/C_{10}DMPO mixtures calculated on the basis of the theoretical model given in refs 14 and 28 using the parameters for the individual lysozyme as reported in ref 24. The surface tension of C_{10}DMPO solutions in phosphate buffer is described satisfactorily by the theoretical model[29] which assumes the internal compressibility of surfactant molecules in the monolayer, that is, change in the orientation (tilt angle) of hydrocarbon chains with respect to the surface. The thin line in Figure 3 shows the C_{10}DMPO theoretical surface tension isotherm calculated with the Langmuir model and internal compressibility taken into consideration.[28,29] Note, in addition to the surface tension and adsorption isotherms, the model also reproduces quite well the rheological characteristics of the mixed protein/surfactant solutions.[28,29]

To describe the adsorption behavior of the mixtures, the parameters of individual components are used, and the only extra parameter is the protein/surfactant intermolecular interaction parameter, similar to the Frumkin parameter, which was taken equal to 1. It is seen from Figure 3 that in the surfactant concentration range below 5×10^{-4} mol/L the theoretical curve agrees satisfactorily with the experimental data. At concentrations above 5×10^{-4} mol/L the theoretical values are somewhat higher than the experimental data. The agreement between theory and experiment could be improved by assuming an adsorption equilibrium constant for the protein (b_P) 1 order of magnitude lower (dashed line).[24] This fact indicates that protein/surfactant hydrophilic complexes are formed at higher C_{10}-DMPO concentrations.

The interaction between a protein and an ionic surfactant obeys a different mechanism. Lysozyme has an isoelectric point at approximately pH 11, and thus at pH 7 it has a net positive charge of 8.[30] At low surfactant concentration, the protein and surfactant molecules begin to form complexes due to electrostatic interactions, where the charges of the protein are being gradually neutralized by the oppositely charged head group of the surfactant. The complexes formed in that manner have a higher surface activity than the pure protein. When SDS concentration is further increased, hydrophobic patches of the protein are then covered by the surfactant making these areas hydrophilic; thus the complex becomes less surface-active.

In Figure 4, the experimental surface tensions for mixtures of 7×10^{-7} mol/L lysozyme/SDS and individual SDS solutions are compared with the theoretical values calculated from the model,[16] using the same parameters as reported in ref 27. The thin solid line corresponds to the formation of complexes by one protein molecule and 8 SDS molecules, assuming that the surface activity of the complex is the same as the one of an individual protein molecule ($b_{PS} = b_P$). Note that for the competitive adsorption of protein and surfactant, the model[14] (which does not imply any complex formation) yields a

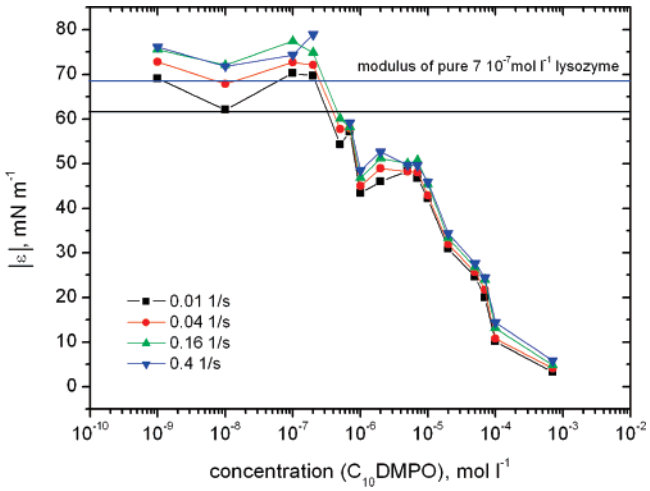

Figure 5. Complex viscoelastic modulus of 7×10^{-7} mol/L lysozyme/C_{10}DMPO versus C_{10}DMPO concentration for different oscillation frequencies.

theoretical dependence which is quite similar to the thin solid line shown in Figure 4, while the bold solid line corresponds to an increase in surface activity of the complex (b_{PS}) by a factor of approximately 10. These theoretical curves agree qualitatively with the experimental data. It is seen that in the concentration range between points A and B, electrostatic bonding of SDS to the protein is very low in view of the low SDS/lysozyme ratio. At SDS concentrations higher than 10^{-6} mol/L (point B), the electrostatic bonding of SDS becomes significant, the hydrophobization of the complex takes place, and results in the increase of its surface activity (BC range in Figure 4). However bearing in mind the fact that at pH 7 the net charge of lysozyme is around 8, charge neutralization is assumed to happen around 10^{-5} mol/L SDS and at higher concentrations hydrophobic interactions also come into play. The decrease of the surface tension for the mixture at concentrations of SDS higher than 10^{-5} mol/L suggests that these complexes are still surface-active. Further increase of SDS concentration leads to the hydrophilization and stepwise solubilization of the complex caused by the dominating hydrophobic interactions (CDE range); however, this does not result in any appreciable surface tension change of the mixture because of the overwhelming excess of free surfactant in this concentration range.

The two isotherms, the one for the mixture and the one for pure SDS, overlap around the critical micelle concentration of SDS (5×10^{-3} mol/L) and suggest an adsorption layer built mainly by free SDS molecules. The appearance of a peak around SDS concentrations of 10^{-3} mol/L was observed also by Green et al.[31] Before the surface tension starts increasing, it remains constant in a short concentration range, from 7×10^{-5} to 2×10^{-4} mol/L, over which the addition of surfactant does not lead to any measurable changes in the surface tension. However, the subsequent γ-increase is an indication for an increased solubility of the lysozyme/SDS complexes. This observation is confirmed by a decrease of the adsorbed amount (from ellipsometry) in the same concentration range (shown below).

Once the competitive adsorption for the two systems investigated has been analyzed in terms of surface tension, one can start the interpretation of the experiments on the dilational rheology. The surface dilational modulus is defined as the increase in surface tension for a small relative increase of the surface area, eq 1. One of the first models characterizing quantitatively the rheology of surfactant mixtures was proposed by Lucassen-Reynders.[40] Later on, the theoretical analysis of

the dilational rheology of surfactant mixtures was improved by Garrett and Joos,[41] who generalized the theory by Lucassen and van den Tempel,[19] and later further developed it in refs 42 and 43. The theoretical results obtained for surfactant mixtures are also applicable to protein/surfactant mixtures; however, such an application should account for adsorption peculiarities of the proteins. The model utilized in this work for the calculations of the experimental dilational elasticity and viscosity is based on a generalized model, the thermodynamic model, which assumes multiple states of the protein molecule in the surface layer and also the internal compressibility of the surfactant surface layer, as summarized in ref 28.

The expression for the complex viscoelastic modulus and applied to a protein/surfactant mixture has the following form:

$$E = \frac{1}{B}\left(\frac{\partial\pi}{\partial \ln \Gamma_S}\right)_{\Gamma_P}\left[\sqrt{\frac{i\omega}{D_S}}\,a_{SS} + \sqrt{\frac{i\omega}{D_P}}\,a_{SP}\frac{\Gamma_P}{\Gamma_S} + \frac{i\omega}{\sqrt{D_S D_P}}(a_{SS}a_{PP} - a_{PS}a_{SP})\right] + \frac{1}{B}\left(\frac{\partial\pi}{\partial \ln \Gamma_P}\right)_{\Gamma_S}\left[\sqrt{\frac{i\omega}{D_S}}\,a_{PS}\frac{\Gamma_S}{\Gamma_P} + \sqrt{\frac{i\omega}{D_P}}\,a_{PP} + \frac{i\omega}{\sqrt{D_S D_P}}(a_{SS}a_{PP} - a_{PS}a_{SP})\right] = \epsilon_R + i\epsilon_I \quad (5)$$

where D_P and D_S are the diffusion coefficients of protein and surfactant, respectively, and $\omega = 2\pi f$ is the angular frequency: and

$$a_{SS} = (\partial\Gamma_S/\partial c_S)_{c_P}$$

$$a_{SP} = (\partial\Gamma_S/\partial c_P)_{c_S}$$

$$a_{PS} = (\partial\Gamma_P/\partial c_S)_{c_P}$$

$$a_{PP} = (\partial\Gamma_P/\partial c_P)_{c_S}$$

$$B = 1 + \sqrt{\frac{i\omega}{D_S}}\,a_{SS} + \sqrt{\frac{i\omega}{D_P}}\,a_{PP} + \frac{i\omega}{\sqrt{D_S D_P}}(a_{SS}a_{PP} - a_{PS}a_{SP})$$

The partial derivatives $a_{ij} = (\partial\Gamma_i/\partial c_j)_{c_i}$ should be determined from the adsorption isotherm. Figures 5 and 6 show the complex viscoelastic modulus and Figures 7 and 8 show its imaginary part as a function of the surfactant concentration obtained for the 7×10^{-7} mol/L lysozyme/C_{10}DMPO and 7×10^{-7} mol/L lysozyme/SDS, respectively, for different oscillation frequencies. The solid straight lines present the modulus for the pure lysozyme with colors corresponding to the colors chosen for the different frequencies. It is seen that for both systems studied with the increase of the oscillation frequency, the complex viscoelastic modulus and the imaginary part ϵ'' increase. Note that since ϵ'' is small, from

$$|\epsilon| = \sqrt{|\epsilon_R|^2 + |\epsilon_I|^2} \quad (6)$$

it follows that $|\epsilon| \approx E$. This rheological behavior is consistent with the behavior observed for pure proteins.[21,32] In general, the elasticity for the mixed system decreases with increasing surfactant concentration. However, for lysozyme/SDS mixtures there are few surfactant concentrations, which produce an increase of the elasticity of the mixed layer with respect to the elasticity for pure lysozyme (see Figure 6).

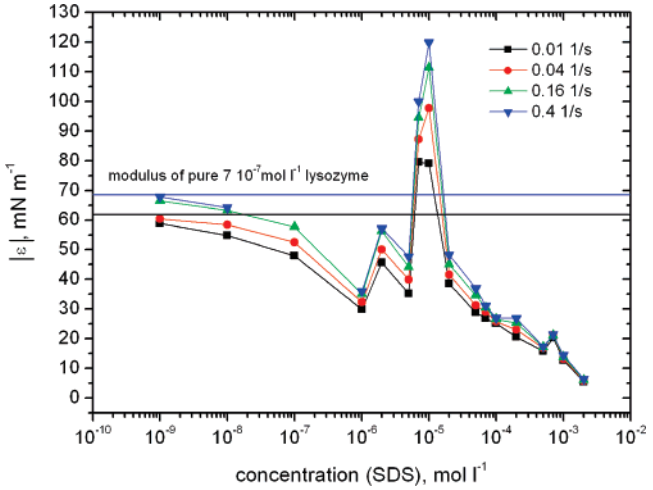

Figure 6. Complex viscoelastic modulus of 7×10^{-7} mol/L lysozyme/SDS versus SDS concentration for different oscillation frequencies.

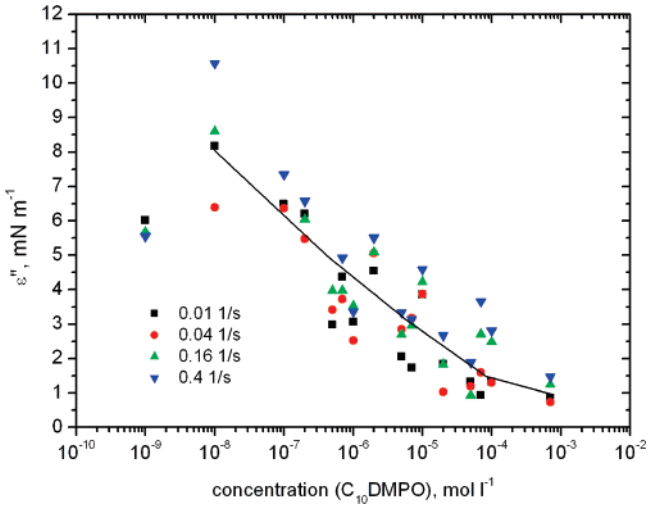

Figure 7. Imaginary part of the complex modulus of 7×10^{-7} mol/L lysozyme/C_{10}DMPO versus C_{10}DMPO concentration for different oscillation frequencies.

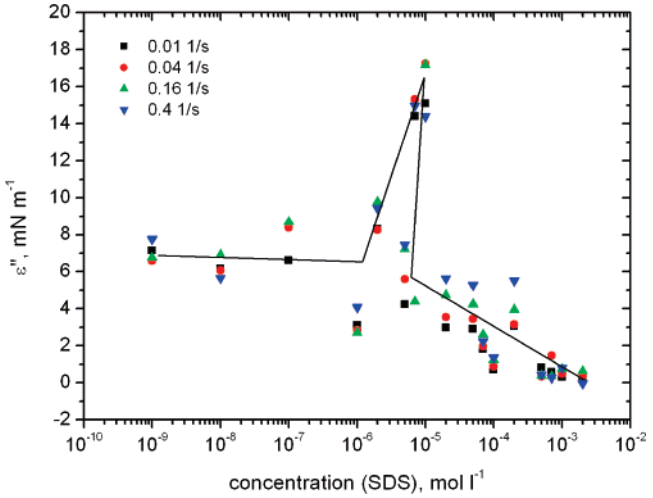

Figure 8. Imaginary part of the complex modulus of 7×10^{-7} mol/L lysozyme/SDS versus SDS concentration for different oscillation frequencies.

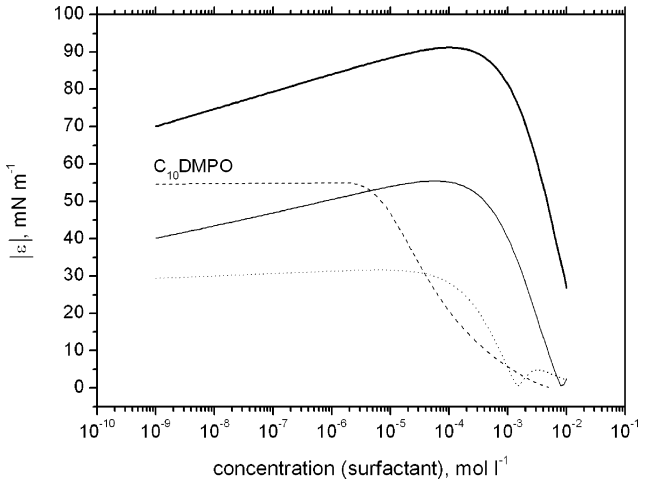

Figure 9. Theoretical dependencies of the complex viscoelastic modulus for 7×10^{-7} mol/L lysozyme/SDS and 7×10^{-7} mol/L lysozyme/C_{10}DMPO versus surfactant concentrations. For details see text.

The dependencies of the dilational modulus on the surfactant concentration for the two mixtures at a fixed oscillation frequency of 0.01 Hz, as calculated using the theoretical model,[28] are shown in Figure 9. For the theoretical calculations, the same set of model parameters was used as for the calculation of equilibrium surface tension curves shown in Figures 3 and 4.[24,27] The model assumes a diffusion mechanism of adsorption for both components and involves therefore the diffusion coefficients.[28] The values are $D = 10^{-12}$ m^2/s for lysozyme and $D = 4 \times 10^{-10}$ m^2/s for each surfactant, which are reasonable values reported in the literature.[28] The dashed line in Figure 9 corresponds to 7×10^{-7} mol/L lysozyme/C_{10}DMPO mixtures, while the other curves are calculated for the 7×10^{-7} mol/L lysozyme/SDS mixtures. The thin solid line is calculated using model parameters corresponding to set 2 from ref 27, where $b_{PS} = 1 \times 10^{-4}$ m^3/mol and the association number is 8. The thick solid line is based on parameters corresponding to set 5, where the adsorption equilibrium constant of the complex is increased to 3×10^{-4} m^3/mol; the dotted line corresponds to parameters of set 6, where the complexation number is increased to 30. The dotted line seems to almost perfectly match the last part of the experimental viscoelastic modulus, (above SDS concentrations 10^{-5} mol/L); however, the maximum revealed from the theoretical fitting occurs at higher SDS concentrations as compared to the experiment. The reason for this discrepancy is not clear. For 7×10^{-7} mol/L lysozyme/C_{10}DMPO, shown in Figures 5 and 9, an increase in C_{10}DMPO concentration lowers the surface coverage by protein molecules. This fact is supported by the permanent decrease of the surface dilational elasticity for the mixed system. The theoretical curve plotted in Figure 9 agrees well with the experimental data shown in Figure 5. As it is seen from the surface tension isotherm, Figure 3, at C_{10}DMPO concentrations above 10^{-4} mol/L, the surfactant concentration is very high compared to the concentration of the protein, which leads to the suppression of further protein adsorption. On the other hand, partial hydrophilization of the protein/surfactant complexes takes place, which acts as an additional hindrance for protein molecules to adsorb and promotes the considerable decrease of the dilational elasticity.

After having discussed the rheological behavior of these two mixed protein/surfactant adsorption layers, we proceed with the analysis of the ellipsometry data. One has to bear in mind, however, that ellipsometry is a useful qualitative technique and for that reason the authors will not seek a high quantitative

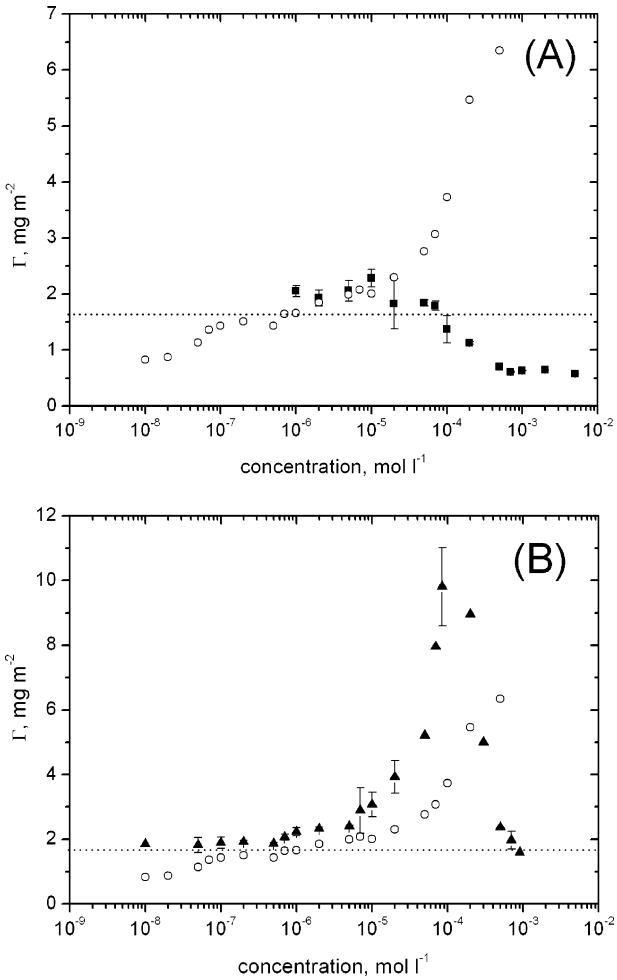

Figure 10. Adsorbed amount for 7×10^{-7} mol/L lysozyme + C_{10}DMPO (A) and 7×10^{-7} mol/L lysozyme + SDS (B) versus surfactant concentration in the case of mixture; (○), pure lysozyme; (■), 7×10^{-7} mol/L lysozyme + C_{10}DMPO; and (▲), 10^{-7} mol/L lysozyme + SDS.

accuracy of the obtained values for the surface concentration. Shown in Figure 10 are the adsorbed amounts for the two mixed layers, respectively, where Figure 10A stands for lysozyme/C_{10}DMPO and Figure 10B stands for lysozyme/SDS. For comparison, the data points for the pure protein from independent measurements are illustrated as well. A dotted line stands for the constant protein amount in the mixed layers corresponding to 7×10^{-7} mol/L concentration.

The experimental dependence of the adsorption from solutions of pure lysozyme is theoretically analyzed in ref 24. It is shown that the model[25,26] provides excellent agreement with the experimental data for the set of parameters used to calculate the theoretical dependencies (cf. Figures 3, 4, and 9). However, at lysozyme concentrations above 10^{-5} mol/L, the model given in ref 25 (in which a monolayer adsorption is assumed) yields adsorption values which are considerably lower than the observed ones. Therefore, a multilayer adsorption model is developed in ref 24 which exhibits exact agreement with the experimental data for pure lysozyme if the number of layers is 4.

The adsorbed amount for lysozyme/C_{10}DMPO is identical to Γ for pure lysozyme and does not change significantly up to 10^{-5} mol/L C_{10}DMPO, Figure 10A. At higher C_{10}DMPO concentrations both species are present at the interface; therefore, the lysozyme adsorption value for the mixed adsorption layer decreases due to the fact that C_{10}DMPO molecules are adsorbed

preferentially. This experimental observation agrees well with the theoretical model.[14]

For lysozyme/SDS mixtures, Figure 10B, the lysozyme adsorption (and surface layer thickness, data not shown) exhibits a maximum at a SDS concentration of 10^{-4} mol/L. This maximum is most probably due to the formation of an adsorbed multilayer. The surface concentration starts gradually increasing at about 10^{-5} M SDS in the mixture, where the hydrophobic interactions come into play and keeps increasing until a maximum at 10^{-4} M SDS is reached. This behavior implies that the lysozyme/SDS complexes obtained after the onset of the hydrophobic interactions are still surface-active and arrive at the interface, resulting in a formation of an adsorbed multilayer. Only after the surfactant concentration becomes too high (higher than 10^{-4}M) do these complexes start solubilizing gradually into the bulk.

Conclusions

In this study, the results of three different experimental methods—tensiometry, ellipsometry, and surface dilational rheology—are presented to characterize the simultaneous adsorption from mixed protein/surfactant solutions. The studies were performed for lysozyme/C_{10}DMPO and lysozyme/SDS mixtures at a fixed lysozyme concentration of 7×10^{-7} mol/L and in a wide range of surfactant concentrations. It is shown that the competitive adsorption depends not only on the concentration of the surfactant in the bulk solution, but also on the surfactant's nature—non-ionic or ionic. For the non-ionic surfactant C_{10}DMPO, the concentration increase results in a monotonous decrease of the equilibrium surface tension, dilational elasticity, and adsorption of lysozyme. For the ionic surfactant SDS, the surface tension exhibits a sharp decrease in the SDS concentration range between 10^{-5} and 10^{-4} mol/L, accompanied by maxima of dilational elasticity and adsorption. This phenomenon can be attributed to the formation (due to the electrostatic interaction) of highly surface-active hydrophobic complexes of lysozyme/SDS. The theoretical model for the dilational viscoelasticity of lysozyme/C_{10}DMPO agrees well with the experimental data; however, for the lysozyme/SDS mixture the agreement between experiment and theory is good only at high SDS concentrations assuming a complexation number 30. At lower SDS concentrations there is a significant discrepancy, which requires additional refinement of the theoretical rheological model for mixed solutions of protein and ionic surfactant.

References and Notes

(1) *Food emulsions and foams, interactions and stability*; Dickinson, E., Rodriguez Patino, J. M., Eds.; Special Publication No. 227; Royal Society of Chemistry, 1999.

(2) Dickinson, E.; Owusu, R. K.; Tan, S.; Williams, A. *J. Food Sci.* **1993**, *58*, 295.

(3) Chen, J. S.; Dickinson, E.; Iveson, G. *Food Struct.* **1993**, *12*, 135.

(4) Murray, B. S.; Ventura, A.; Lallemant, C. *Colloids Surf., A* **1998**, *143*, 211.

(5) Bos, M. A.; van Vliet, T. *Adv. Colloid Interface Sci.* **2001**, *91*, 437.

(6) Mackie, A. R.; Gunning, A. P.; Ridout, M. J.; Wilde P. J.; Rodriguez Patino, J. *Biomacromolecules* **2001**, *2*, 1001.

(7) Mackie, A. R.; Gunning, A. P.; Pugnaloni, L. A.; Dickinson, E.; Wilde, P. J.; Morris, V. J. *Langmuir* **2003**, *19*, 6032.

(8) Mackie, A. R.; Gunning, A. P.; Ridout, M. J.; Wilde, P. J.; Morris, V. J. *Langmuir* **2001**, *17*, 6593.

(9) Ferri, J. K.; Dong, W.-F.; Miller, R.; Möhwald, H. *Macromolecules* **2006**, *39*, 1532.

(10) Fainerman, V. B.; Leser, M. E.; Michel, M.; Lucassen-Reynders, E. H.; Miller, R. *J. Phys. Chem. B* **2005**, *109*, 9672.

(11) Kazakov, V. N.; Sinyachenko, O. V.; Fainerman, V. B.; Pison, U.; Miller, R. Dynamic Surface Tension of Biological Liquids in Medicine. In *Studies in Interface Science*; Möbius, D., Miller, R., Eds.; Elsevier: Amsterdam, 2000; Vol. 8.

(12) Dickinson, E. *Colloids Surf., B* **1999**, *15*, 161.

(13) Mackie, A. R.; Gunning, A. P.; Wilde, P. J.; Morris, V. J. *J. Colloid Interface Sci.* **1999**, *210*, 157.

(14) Fainerman, V. B.; Zholob, S. A.; Leser, M.; Michel, M.; Miller, R. *J. Colloid Interface Sci.* **2004**, *274*, 496.

(15) Miller, R.; Fainerman, V. B.; Makievski, A. V.; Krägel, J.; Grigoriev, D. O.; Kazakov, V. N.; Sinyachenko, O. V. *Adv. Colloid Interface Sci.* **2000**, *86*, 39.

(16) Fainerman, V. B.; Zholob, S. A.; Leser, M. E.; Michel, M.; Miller, R. *J. Phys. Chem.* **2004**, *108*, 16780.

(17) Loglio, G.; Pandolfini, P.; Miller, R.; Makievski, A. V.; Ravera, F.; Ferrari, M.; Liggieri, L. Drop and bubble shape analysis as tool for dilational rheology studies of interfacial layers. In *Novel Methods to Study Interfacial Layers, Studies in Interface Science*; Möbius, D., Miller, R., Eds.; Elsevier: Amsterdam, 2001; Vol. 11.

(18) Lucassen, J.; Hansen, R. S. *J. Colloid Interface Sci.* **1967**, *23*, 319.

(19) Lucassen, J.; van den Tempel, M. *Chem. Eng. Sci.* **1972**, *27*, 1283.

(20) Lucassen, J.; van den Tempel, M. *J. Colloid Interface Sci.* **1972**, *41*, 491.

(21) Benjamins, J.; Lyklema, J.; Lucassen-Reynders, E. H. *Langmuir* **2006**, *22*, 6181.

(22) Harke, M.; Teppner, R.; Schulz, O.; Orendi, H.; Motschmann, H. *Rev. Sci. Instrum.* **1997**, *8*, 68.

(23) Motschmann, H.; Teppner, R. Ellipsometry in Interface Science. In *Novel Methods to Study Interfacial Layers, Studies in Interface Science*; Möbius, D., Miller, R., Eds.; Elsevier: Amsterdam, 2001; Vol. 11.

(24) Grigoriev, D. O.; Fainerman, V. B.; Makievski, A. V.; Krägel, J.; Wüstneck, R.; Miller, R. *J. Colloid Interface Sci.* **2002**, *253*, 257.

(25) Alahverdjieva, V. S.; Grigoriev, D. O.; Ferri, J. K.; Fainerman, V. B.; Aksenenko, E. V.; Leser, M. E.; Michel M.; Miller, R. *Colloids Surf., A* **2008**, doi: 10.1016/j.colsurfa.2007.12.031.

(26) Fainerman, V. B.; Lucassen-Reynders, E. H.; Miller, R. *Adv. Colloid Interface Sci.* **2003**, *106*, 237.

(27) Lucassen-Reynders, E. H.; Fainerman, V. B.; Miller, R. *J. Phys. Chem.* **2004**, *108*, 9173.

(28) Alahverdjieva, V. S.; Fainerman, V. B.; Aksenenko, E. V.; Leser, M. E.; Miller, R. *Colloids Surf., A* **2008**, doi: 10.1016/j.colsurfa.2007.11.062.

(29) Aksenenko, E. V.; Kovalchuk, V. I.; Fainerman, V. B.; Miller, R. *Adv. Colloid Interface Sci.* **2006**, *122*, 57.

(30) Fainerman, V. B.; Kovalchuk, V. I.; Aksenenko, E. V.; Michel, M.; Leser, M. E.; Miller, R. *J. Phys. Chem.* **2004**, *108*, 13700.

(31) Lad, M. D.; Ledger, V. M.; Briggs, B.; Green, R. G.; Frazier, R. A. *Langmuir* **2003**, *19*, 5098.

(32) Green, R. G.; Su, T. J.; Joy, H.; Lu, J. R. *Langmuir* **2000**, *16*, 5797.

(33) Maldonado-Valderrama, J.; Fainerman, V. B.; Galvez-Ruiz, M. J.; Martin-Rodriguez, A.; Cabrerizo-Vilchez, M. A.; Miller, R. *J. Phys. Chem. B* **2005**, *109*, 17608.

(34) Benjamins, J.; Lucassen-Reynders, E. H. In Proteins at Liquid Interfaces; Möbius, D., Miller, R., Eds.; Elsevier: Amsterdam, The Netherlands, 1998.

(35) Mellema, M.; Clark, D. C.; Husband, F. A.; Mackie, A. R. *Langmuir* **1998**, *14*, 1753.

(36) Leser, M. E.; Acquistapace, S.; Cagna, A.; Makievski, A. V.; Miller, R. *Colloids Surf., A* **2005**, *261*, 25.

(37) De Feijter, J. A.; Benjamins, J.; Veer, F. A. *Biopolymers* **1978**, *17*, 1759.

(38) Sundaram, S.; Ferri, J. K.; Vollhardt, D.; Stebe, K. J. *Langmuir* **1998**, *14*, 1208.

(39) Fainerman, V. B.; Miller, R. *Langmuir* **1999**, *15*, 1812.

(40) Miller, R.; Fainerman, V. B.; Leser, M. E.; Michel, M. *Curr. Opin. Colloid Interface Sci.* **2004**, *9*, 350.

(41) Lucassen-Reynders, E. H. *J. Colloid Interface Sci.* **1973**, *42*, 573.

(42) Garrett, P. R.; Joos, P. J. *J. Chem. Soc., Faraday Trans.* **1976**, *72*, 2161.

(43) Jiang, Q.; Valentini, J. E.; Chiew, Y. C. *J. Colloid Interface Sci.* **1995**, *174*, 268.

(44) Joos, P. *Dynamic Surface Phenomena*; VSP: Utrecht, 1999.

(45) Fainerman, V. B.; Miller, R.; Kovalchuk, V. I. *J. Phys. Chem. B* **2003**, *107*, 6119.

(46) Fainerman, V. B.; Zholob, S. A.; Leser, M.; Michel, M.; Miller, R. *J. Colloid Interface Sci.* **2004**, *274*, 496.